Gravitational waves from phase transitions in the early Universe

Workshop seminar, 20.06.2017

- The early Universe might have undergone multiple phase transitions (QCD, electroweak, GUT...)
- A first order PT leads to a stochastic gravitational wave background.
- Complementary to collider experiments as probe of new physics.

1 The (hydro)dynamics of a phase transition [1]

- The properties of the phase transition are captured by the free-energy $\mathcal{F}$ ($\equiv V_{\text{eff}}$) (recall $\mathcal{F} = U - TS$)

$$\mathcal{F} = V_0 + T \sum_i \int \frac{d^3k}{(2\pi)^3} \log\left(1 \mp e^{-\sqrt{k^2+m_i^2}/T}\right).$$

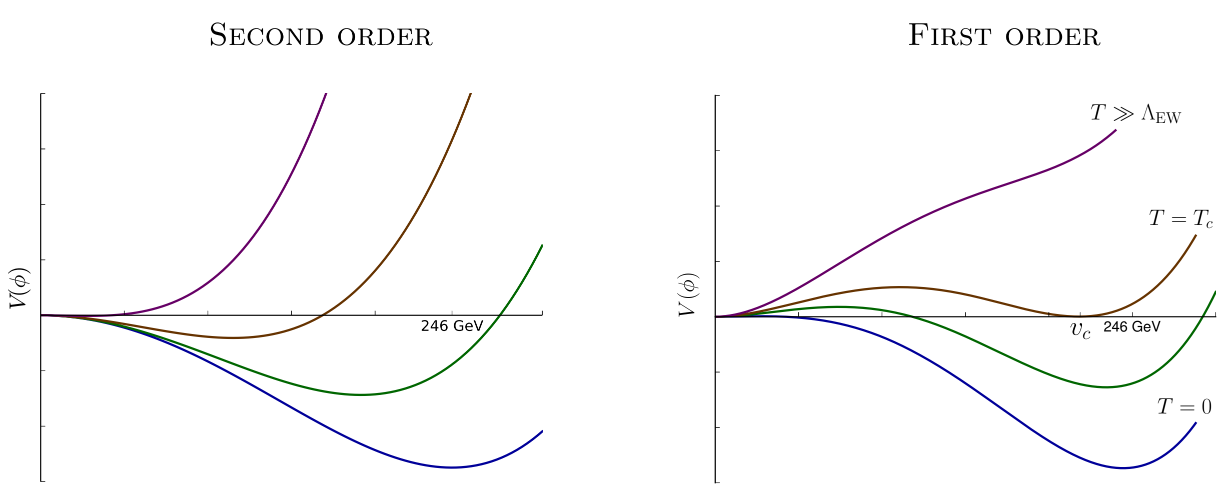

Figure 1: Effective thermal potential for the Higgs field describing a second and first order electroweak phase transition.

- A barrier between two minima induces a first order phase transition $\Rightarrow$ proceeds via bubble nucleation, with rate per unit volume

$$\Gamma/\mathcal{V} \simeq T^4 e^{-S_3/T}.$$

$S_3 \equiv$ thermal effective action obtainable from $\mathcal{F}$

- Expansion of spherical bubble does not generate GW (no quadrupole).
Bubble collisions break spherical symmetry.
GW sourced by:
  - kinetic energy of scalar fields in expanding bubble wall;
  - acoustic oscillations in the fluid;
  - turbulence.

- Envelope approx. $\rightarrow$ consider only expanding uncollided shells
Not good for thermal transitions (fluid oscillations, and possibly turbulence, continue to source GW in collision regions).

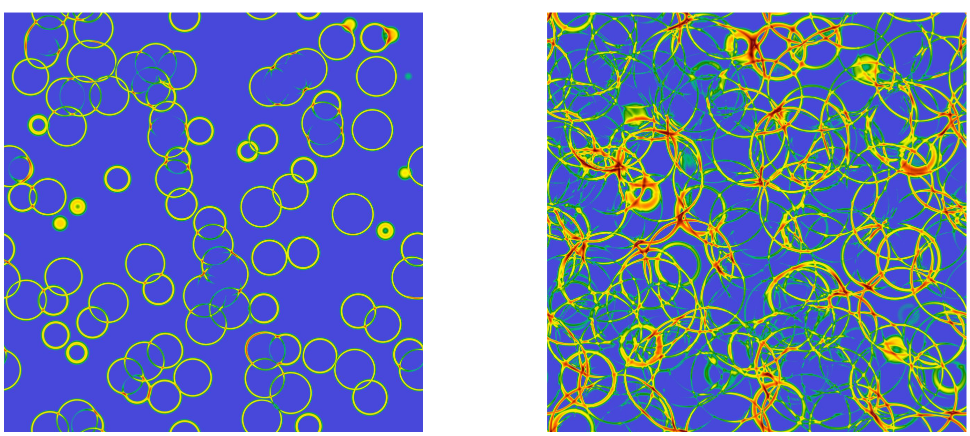

Figure 2: Simulation of bubble collisions, from arXiv:1504.03291.

- Modelling fluid as a relativistic gas $\Rightarrow$ pressure and energy density read

$$p = \frac{\pi^2}{90} g_* T^4 - \epsilon, \qquad u \equiv T\frac{\partial p}{\partial T} - p = \frac{\pi^2}{30} g_* T^4 + \epsilon,$$

where

$$\begin{aligned} p &= -\mathcal{F}, \\ \epsilon &\equiv \text{ energy of false-vacuum} = \frac{1}{4}\left(u - 3p\right). \end{aligned}$$

- An important parameter for GW production:

$$\alpha \equiv \frac{\epsilon}{\rho_{\rm rad}} = \frac{30\,\epsilon}{g_* T^4},$$

the amount of energy released by phase transition which **can** be converted into kinetic energy (normalized to total radiation energy in the fluid).

- Another relevant parameter is the duration of the phase transition. Expand the nucleation rate around the so-called finalization time t_*:

$$\Gamma = \Gamma_*\, e^{-\beta\,(t-t_*)}.$$

Adiabatic expansion $\Rightarrow dT/dt = -TH$, so

$$\frac{\beta}{H_*} = T_* \left.\frac{d\left(S_3/T\right)}{dT}\right|_{T_*}.$$

Large β: PT is "nucleation dominated" $\Rightarrow$ small bubbles $\Rightarrow$ small GW signal Small β: transition completed mainly due to bubble expansion $\Rightarrow$ large bubbles, large GW signal.

- Average bubble size $R \sim v_w/\beta$.

- For the wall velocity, solve EoM coupled to hydrodynamic equations (continuity of $T_{\mu\nu}$ along bubble wall). The EoM has the form

$$\Box\phi + \frac{\partial \mathcal{F}}{\partial \phi} + \underbrace{\sum_i \frac{dm_i^2}{d\phi} \int \frac{d^3k}{2E_i\,(2\pi)^3} \delta f_i}_{\substack{\text{friction term} \\ \text{need to solve Boltzmann eqs.}}} = 0.$$

2 Gravitational wave spectrum [2, 3]

- Many independent bubble collisions $\Rightarrow$ multiple uncorrelated sources $\Rightarrow$ stochastic GW background
- GW energy density in terms of metric perturbations h_{ij}:

$$\rho_{\rm GW} = \frac{1}{32\pi G}\langle \dot{h}_{ij}(\mathbf{x})\dot{h}^{ij}(\mathbf{x})\rangle.$$

- Fourier transforming and defining the power spectrum

$$\langle \dot{h}_{ij}(\mathbf{k},t)\,\dot{h}^{ij}(\mathbf{k}',t)\rangle = (2\pi)^3\delta(\mathbf{k}+\mathbf{k}')P_{\dot{h}}(k,t)$$

yields

$$\frac{d\rho_{\rm GW}}{d\log k} = \frac{1}{32\pi G}\frac{k^3}{2\pi^2}P_{\dot{h}}(k,t).$$

- Given the energy-momentum tensor τ_{ij}, GW equation reads:

$$\Box h_{ij} = 16\pi G \lambda_{ij}{}^{kl}\tau_{kl},$$

$\lambda_{ij}{}^{kl} \equiv$ projector onto transverse traceless modes.

$$h_{ij}(\mathbf{k},t) = 16\pi G\int dt'\;\frac{\sin[k(t-t')]}{k}\lambda_{ij}{}^{kl}\tau_{kl}(\mathbf{k},t').$$

- We can define

$$\lambda_{ij,kl}\langle \tau^{ij}(\mathbf{k},t)\,\tau^{kl}(\mathbf{k},t')\rangle \equiv (\kappa\epsilon)^2R^3\;\underbrace{\widetilde{\Pi}(k,t-t')}_{\text{dimensionless}}\,(2\pi)^3\delta(\mathbf{k}-\mathbf{k}'),$$

$\kappa \equiv \rho_{\rm kin}/\epsilon =$ efficiency in converting released energy ϵ into kinetic energy. After some manipulation

$$P_{\dot{h}} = (16\pi G)^2\,(\kappa\epsilon)^2\,R^3\,\tau\,k^{-1}\int dz\frac{\cos z}{2}\widetilde{\Pi}(kR,z)$$

where $\tau \equiv$ source duration, $R \equiv$ natural length scale $\simeq$ average bubble size.

- Writing $G = \dfrac{3H_*^2}{8\pi\rho_c}$ and recalling $\rho_c \approx \rho_{\rm tot} = \rho_{\rm rad} + \epsilon = (1+\alpha)\,\rho_{\rm rad}$,

$$\Omega_{\rm GW} \equiv \frac{\rho_{\rm GW}}{\rho_c} = \left(\frac{\kappa\alpha}{1+\alpha}\right)^2 (R\,H_*)\,(\tau H_*)\,\widetilde{\Omega}_{\rm GW}.$$

2.1 Properties of the spectrum

- $R \sim \beta^{-1}$.
  The lifetime of the source depends on its nature.
  Envelope approximation $\Rightarrow \tau \sim \beta$ (kinetic energy in bubble walls).
  Acoustic oscillations and turbulence are longer lived: $\tau \sim H_*^{-1}$.

$$\frac{\Omega_{\rm GW}^{\rm long\ lived}}{\Omega_{\rm GW}^{\rm envelope}} \sim \frac{\beta}{H_*} \sim \mathcal{O}(10^2)$$

  For phase transitions at high T, envelope approx. greatly underestimates the spectrum.

- At large scales (low frequency) the sources are causally disconnected, so signal is white noise,

$$\Omega_{\rm GW}(k \lesssim k_*) \propto k^3.$$

  Since total GW energy must be finite, spectrum must decrease for $k \gtrsim k_*$. The exact behaviour depends on the particularities of the source.

- k_* denotes the characteristic frequency of the source.
  For a phase transition, $k_* \sim \beta$.

2.2 Red-shifted spectrum

- Adiabatic expansion: $S \propto a^3\, g_s\, T^3 \equiv$ constant,

$$\frac{a_*}{a_0} = \left(\frac{g_{s0}}{g_{s*}}\right)^{1/3} \frac{T_0}{T_*}.$$

- If characteristic frequency is originally f_*, the redshifted frequency today is

$$f = f_* \left(\frac{a_*}{a_0}\right) = \sqrt{\frac{\pi^2}{90}} \frac{T_0\, g_{s0}^{1/3}}{m_{\rm Pl}} (g_{s*})^{1/6}\, T_* \left(\frac{f_*}{H_*}\right)$$

  where we used $H_* = \sqrt{\frac{\pi^2 g_*}{90}} \frac{T_*^2}{m_{\rm Pl}}$ and $m_{\rm Pl} = (8\pi G)^{-1/2} \approx 2.435 \times 10^{18}$ GeV.

- Plugging in values, $T_0 \approx 2.725\,K \approx 2.348 \times 10^{-13}$ GeV and $g_0 \approx 3.91$,

$$f \simeq 16.5 \times 10^{-3} \text{ mHz } \left(\frac{g_{s*}}{100}\right)^{1/6} \frac{T_*}{100 \text{ GeV}} \left(\frac{f_*}{H_*}\right).$$

- The energy density scales as a^{-4}, so (recall $\rho_c \propto H^2$)

$$\Omega_{\rm GW} = \frac{\rho_{\rm GW}}{\rho_c} = \Omega_{\rm GW*} \underbrace{\left(\frac{\rho_{\rm GW}}{\rho_{\rm GW*}}\right)}_{\left(\frac{a_*}{a_0}\right)^4} \underbrace{\left(\frac{\rho_{c*}}{\rho_c}\right)}_{\left(\frac{H_*}{H_0}\right)^2}.$$

- Putting everything together and writing $H_0 \equiv h{\times}100 \, \frac{\text{km}}{\text{s Mpc}}$ ($h \approx 0.67$–0.70),

$$h^2\Omega_{\rm GW}(f) = 1.67 \times 10^{-5} \left(\frac{g_*}{100}\right)^{-1/3} \left(\frac{\kappa\alpha}{1+\alpha}\right)^2 \left(\frac{H_*}{\beta}\right) (\tau H_*)\, v_w\, \widetilde{\Omega}_{\rm GW}(v_w, f).$$

- The precise value for f_* and frequency dependence of $\widetilde{\Omega}_{\rm GW}$ are best determined by numerical simulations. A summary of our best-knowledge so far has been compiled in the eLISA Working Group study, arXiv:1512.06239 [4].

3 Observational aspects

- Red-shifted frequency of GW from EW transition lies in the mHz region. In the detection band of LISA.
- Three-armed space-based interferometer, $L \sim 10^6$ km.
- Astrophysical foreground:
  - Merging neutron star and stellar BH: can be separately identified and subtracted
  - Overwhelming galactic foreground (binary stars in Milky Way) anisotropic! $\Rightarrow$ can be subtracted!
  - Irreducible background from extragalactic binary stars (WD pairs) For $f \lesssim 50$ mHz: too many sources to be resolved and subtracted one-by-one.

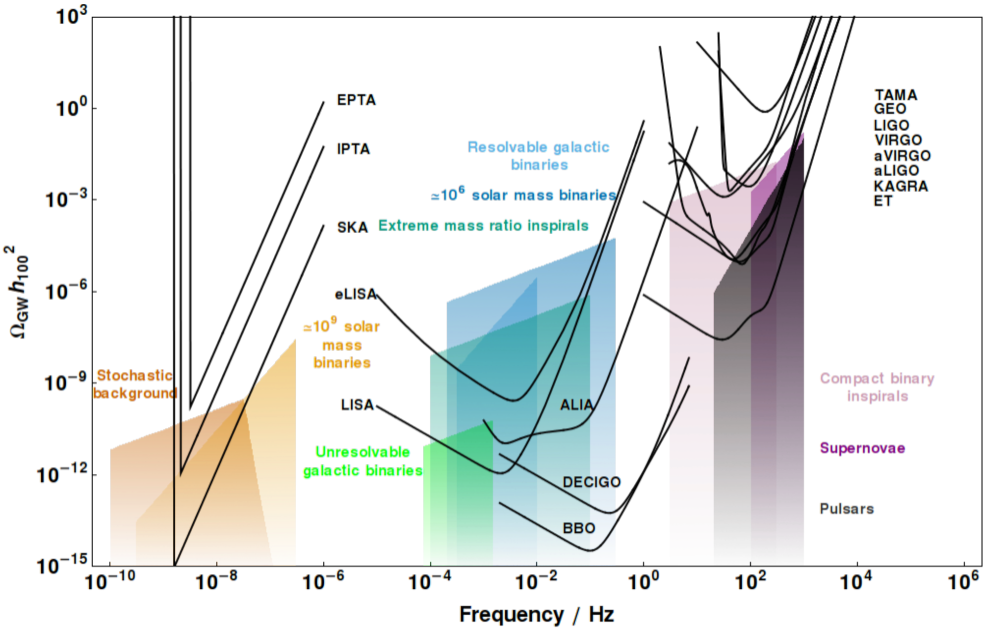

Figure 3: Sensitivity curves for various detectors, from arXiv:1408.0740.

References

[1] J. R. Espinosa, T. Konstandin, J. M. No and G. Servant, "Energy Budget of Cosmological First-order Phase Transitions," JCAP **1006** (2010) 028 [arXiv:1004.4187 [hep-ph]].

[2] M. Hindmarsh, S. J. Huber, K. Rummukainen and D. J. Weir, "Numerical simulations of acoustically generated gravitational waves at a first order phase transition," Phys. Rev. D **92** (2015) no.12, 123009 [arXiv:1504.03291 [astro-ph.CO]].

[3] C. Grojean and G. Servant, "Gravitational Waves from Phase Transitions at the Electroweak Scale and Beyond," Phys. Rev. D **75** (2007) 043507 [hep-ph/0607107].

[4] C. Caprini *et al.*, "Science with the space-based interferometer eLISA. II: Gravitational waves from cosmological phase transitions," JCAP **1604** (2016) no.04, 001 [arXiv:1512.06239 [astro-ph.CO]].